A Nucleotide-dependent Molecular Switch Controls ATP Binding at the C-terminal Domain of Hsp90

N-TERMINAL NUCLEOTIDE BINDING UNMASKS A C-TERMINAL BINDING POCKET*

Csaba Söti, Attila Rácz, and Péter Csermely‡

From the Department of Medical Chemistry, Semmelweis University, P. O. Box 260, Budapest H-1444, Hungary

In vivo function of the molecular chaperone Hsp90 is ATP-dependent and requires the full-length protein. Our earlier studies predicted a second C-terminal ATP-binding site in Hsp90. By applying direct biochemical approaches, we mapped two ATP-binding sites and unveiled the C-terminal ATP-binding site as the first example of a cryptic chaperone nucleotide-binding site, which is opened by occupancy of the N-terminal site. We identified an N-terminal γ−phosphate-binding motif in the middle domain of Hsp90 similar to other GHKL family members. This motif is adjacent to the phosphate-binding region of the C-terminal ATP-binding site. Whereas novobiocin disrupts both C- and N-terminal nucleotide binding, we found a selective C-terminal nucleotide competitor, cisplatin, that strengthens the Hsp90-Hsp70 complex leaving the Hsp90-p23 complex intact. Cisplatin may provide a pharmacological tool to dissect C- and N-terminal nucleotide binding of Hsp90. A model is proposed on the interactions of the two nucleotide-binding domains and the charged region of Hsp90.

The 90-kDa heat shock protein (Hsp90)[1] is a central part of a chaperone meshwork, the foldosome, specifically chaperoning molecules involved in signal transduction and cell cycle regulation (1–3). Hsp90 is an ATP-binding chaperone (4, 5). Assembly of the Hsp90-client protein complexes requires ATP (6, 7), and ATP binding induces a conformational change in Hsp90 (8, 9). Moreover, ATP binding and hydrolysis are essential for the *in vivo* function of the chaperone (10, 11).

Crystallization of the N-terminal domain uncovered a Bergerat-type ATP-binding fold (12), sharing a similar tertiary structure with the so-called GHKL family members, bacterial type II topoisomerase gyrase B and the mismatch repair protein MutL (13). Geldanamycin (GA) (14) and radicicol (15, 16) are highly specific antagonists of the N-terminal ATP-binding site. These natural antitumor antibiotics abolish Hsp90-dependent folding of immature client proteins and direct them to proteolysis (17, 18). Interestingly, the gyrase inhibitor, novobiocin (NB), also compromises Hsp90 function similarly to GA

(19), but although its binding site in the gyrase overlaps with the N-terminal ATP-binding site (13), that in Hsp90 is located in its C terminus (19, 20).

Our earlier studies suggested that a second ATP-binding site exists in the C-terminal domain of Hsp90 (2, 4, 21), and observations with possibly similar explanations have been reported by others (5, 22). During the preparation of this article, a paper by Neckers and co-workers (20) reported that a C-terminal fragment (aa 383–731, to help direct comparison, if not otherwise indicated, all Hsp90 sequences are given as sequences of human Hsp90α) indeed is able to bind to ATP-Sepharose in a novobiocin-sensitive manner. Deletion of amino acids 660–680 abolished both ATP and novobiocin binding, indicating this segment as part of a novel ATP-binding site.

In the present study we have mapped the ATP-binding sites by direct biochemical approaches. Our results suggest that a residue in the middle domain interacts with the N-terminally bound ATP, pointing out the existence of a γ-phosphate-binding site to the analogy of the GHKL family members. More importantly, we could also identify a cryptic C-terminal, cisplatin-sensitive ATP-binding site, demonstrate that novobiocin inhibits both sites, and show that the N- and C-terminal ATP-binding sites interact in a very sophisticated way, supporting the existence of two cooperatively interacting parts of the chaperone.

EXPERIMENTAL PROCEDURES

Hsp90 Purification—Rat liver Hsp90 was purified as described earlier (23). Human Hsp90α was expressed from a pMAL-cRI/human Hsp90α-(3–731) plasmid in *Escherichia coli* as a maltose-binding protein fusion partner and was purified on an amylose resin (PerkinElmer Life Sciences). After proteolytic removal of the maltose-binding protein tag, the protein was further purified on a Bioscale UNO Q column (Bio-Rad). The purified protein was fully soluble and active in chaperone assays.

[α-^{32}P]ATP Photocross-linking—Photoaffinity labeling was performed according to Biswas and Kornberg (24). Three μg of Hsp90 were incubated in the presence of 200 μM ATP (containing 5–10 μCi of [α-^{32}P]ATP, PerkinElmer Life Sciences) in 50 mM Hepes, pH 7.4, 50 mM KCl, 2 mM EDTA, or 5–10 mM MgCl$_2$, 30 min at 37 °C, after a 30-min preincubation in the absence or presence of inhibitors. Samples were placed in an aluminum block on ice and were irradiated in a UV Stratalinker from a distance of 10 cm for 30 min. Non-bound radionuclide was separated on SDS-PAGE, and the gel was analyzed by silver staining, drying, and autoradiography.

Far UV Circular Dichroism Measurements—CD spectra were recorded on a Jobin-Yvon VI dichrograph in a thermostated 0.01-cm path length cylindrical quartz cell at 25 °C. Samples contained 0.3–0.5 mg/ml Hsp90 in 25 mM Hepes, pH 7.4. Final concentrations of geldanamycin (Invitrogen) and ATP were 18 μM and 1 mM, respectively. In this case geldanamycin was diluted from an acetonitrile stock (instead of Me$_2$SO), which did not influence the effectivity of the compound in the ATP affinity cleavage reaction. Mean residue ellipticities were calculated using a mean residue molecular mass of 115.

γ-Phosphate-linked ATP-Sepharose Binding—Binding assays to

[1] The abbreviations used are: Hsp90, 90-kDa heat shock protein; Hsp, heat shock protein; Me$_2$SO, dimethyl sulfoxide; CP, cisplatin; GA, geldanamycin; NB, novobiocin; aa, amino acid; ATPγS, adenosine 5′-*O*-(thiotriphosphate); AMP-PNP, adenosine 5′-($β$,γ-imino)triphosphate.

γ-phosphate-linked ATP-Sepharose (Upstate Biotechnology, Inc.) were performed according to Grenert *et al.* (6) with minor modifications. 5 μg of rat Hsp90 was preincubated with the indicated additions on ice for 1 h in 200 μl of HKMN buffer (20 mM Hepes, 50 mM KCl, 6 mM MgCl₂, 0.01% Nonidet P-40, pH 7.5). In the case of ATP competition, samples contained an ATP regeneration system (10 mM creatine phosphate and 20 units/ml creatine kinase). Finally, 25 μl γ-phosphate-linked ATP-Sepharose was added, and tubes were incubated at 37 °C for 30 min with frequent agitation, and then the resin was pelleted and washed twice with HKMN buffer and analyzed by SDS-PAGE.

Oxidative Nucleotide Affinity Cleavage—Affinity cleavage reactions were performed as described by Alonso and Rubio (25). Two μg of Hsp90 were incubated for 30 min at 37 °C in the presence of 20 mM Hepes, 50 mM KCl, pH 7.4, 0.5 mM FeCl₃, 30 mM ascorbate, and 1 mM nucleotides, if not otherwise indicated. In the majority of experiments, samples contained an ATP regeneration system (10 mM creatine phosphate and 20 units/ml creatine kinase). In competition experiments a 15-min to 1-h preincubation was done with the indicated additions. Fragmentation was assessed by SDS-PAGE and silver staining or immunoblotting with different antibodies (26; Institute of Immunology Ltd., Tokyo, Japan) directed against the N terminus (K41218, Hsp90α/β-reactive, PA3–012, Hsp90β-specific; Affinity Bioreagents) or the C terminus (K41007, Hsp90α-specific and K3725B, Hsp90β-specific) of Hsp90.

Nitrocellulose Filter Binding Assay—ATP binding to Hsp90 was analyzed by retaining the protein-bound ATP on a nitrocellulose filter (TransBlot, Bio-Rad) as described by Wong and Lohman (27) and Ban *et al.* (28). The nitrocellulose membrane (protein binding capacity was determined to be 4.5–5 μg/well) was equilibrated for a minimum of 2 h in binding buffer (40 mM Hepes, 100 mM KCl, 1 mM MgCl₂, pH 7.5) at 4 °C. Hsp90 was preincubated in the absence or presence of 60 μM radicicol or 36 μM geldanamycin for 1 h in binding buffer on ice, and then Mg-[α-³²P]ATP (10⁷–2 × 10⁷ cpm/sample) was added at the indicated concentrations, and samples were incubated for an additional 20 min at 37 °C. 30-μl aliquots (containing 4.2 μg of Hsp90 or thioredoxin as control) in triplicate were filtered through the wells of the PR 648 Slot Blot Filtration Manifold (Hoefer) and immediately washed once with 200 μl of ice-cold binding buffer. Blots were rinsed and dried, and bound radioactivity was assessed using a PhosphorImager. Protein binding to the membrane was checked in samples containing no radioactivity and found to be constant, irrespective of the ATP/radicicol/geldanamycin concentration. Accurate stoichiometric determination of ATP binding was done by liquid scintillation counting and was compared with the total radioactivity of the samples. Nucleotide binding of both thioredoxin and nitrocellulose was negligible.

p23 Binding Assay—Binding of p23 was assessed according to Sullivan *et al.* (9). 10 μg of Hsp90 and 4 μg of p23 were preincubated in the presence of the indicated inhibitors at 4 °C for 30 min, in 10 mM Hepes, pH 7.5, 50 mM KCl, 5 mM MgCl₂, 1 mM dithiothreitol, and then samples were supplemented with 5 mM ATP or 0.5 mM ATPγS and an ATP regeneration system (10 mM creatine phosphate and 20 units/ml creatine kinase) and/or 20 mM molybdate and incubated for 60 min at 37 °C. Immunoprecipitation was performed with the JJ3 anti-p23 antibody. Pellets were washed three times with binding buffer and analyzed by SDS-PAGE.

Hsp90/Hsp70 Co-precipitation—Jurkat cells were cultured in RPMI medium supplemented with 10% fetal bovine serum, 2 mM L-glutamine, 100 units/ml penicillin, and 100 μg/ml streptomycin. Cells were transferred into serum-free medium and incubated either with 1.8 μM geldanamycin, 100 μM cisplatin (Sigma) or 1 mM novobiocin (Sigma) for 3 h. After washing with phosphate-buffered saline, cells were Dounce-homogenized in 10 mM Hepes, 1 mM phenylmethylsulfonyl fluoride, 5 μg/ml leupeptin, 0.7 μg/ml pepstatin A, pH 7.5 (lysis buffer), on ice and then clarified by centrifugation. Hsp70 was immunoprecipitated with the SPA-810 antibody (StressGen). Pellets were washed three times with lysis buffer + 50 mM KCl and analyzed by SDS-PAGE and immunoblotting with anti-Hsp90 and anti-Hsp70 antibodies.

Determination of the N-terminal γ-Phosphate-binding Motif of Hsp90—First, prokaryotic (sp P10413 and sp P46208), yeast (sp P02829), plant (sp P36181 and sp P33126), protozoon (tr O76257), fruit fly (sp P02828), avian (sp P11501), murine (sp P34058 and sp P07901), and human (sp P07901 and sp P08238) Hsp90 as well as fruit fly (tr Q9V9D1) and human (sp Q12931) Trap1 sequences were screened for conserved Lys residues by multiple sequence alignment with ClustalW 1.74 (www.ch.embnet.org/software/ClustalW.html), using default values. Parallel with this, yeast, murine, and human Hsp90 sequences as well as the sequences of *E. coli* gyrase B (sp P06982) and MutL (sp P23367) proteins were sent to the Predict Protein Server (dodo.cpmc.columbia.edu/predictprotein/), and secondary structure pre-

dictions were made according to Rost and Sander (29, 30) with default values. Comparing the predicted structures with the known crystal structures using the coordinates of the Protein Data Bank (MutL, 1BKN; gyrase B, 1EI1; and human Hsp90α, 1YET), the overall accuracy was estimated as 81.6, 71.3, and 87.3% for MutL, GyrB and human Hsp90α, respectively, which shows a highly accurate prediction level. To find possible γ-phosphate-binding sites, segments containing conserved lysines with conserved Gln or Asn residues in the preceding 2–7 amino acid regions were selected, and a manual alignment between Hsp90 and MutL/GyrB was performed based on the known ATP-binding motifs and crystal structure of the GHKL family (13). Finally, the preselected γ-phosphate-binding sites were scored using secondary structure fitting as a matching criterion.

RESULTS

Nucleotide Affinity Cleavage Identifies Two ATP-binding Sites in Hsp90—Because exact three-dimensional structural studies of Hsp90 have been confined to the N-terminal domain (12, 14), we decided to study the Hsp90-ATP interactions in solution on the whole protein. A smart and reliable but nevertheless seldom applied form of ligand-binding site mapping is the iron-catalyzed chemical proteolysis, where iron is targeted with a chelating molecule that specifically binds to the protein. Oxidation of the liganded Fe²⁺ by O₂ produces hydroxyl radicals, which in turn attack and fragment the polypeptide backbone at the binding site. This reaction has been used to map the metal-isocitrate-binding site of NADP-specific isocitrate dehydrogenase (31), and the ATP-binding site of carbamoyl-phosphate synthetase (25; Fig. 1*A*). Fig. 1*B* shows the result of an Hsp90 ATP-affinity cleavage reaction. Unliganded iron produces two specific fragments (Fig. 1*B, 2nd lane*), suggesting the presence of a divalent cation-binding site. ADP and ATP generate several fragments, clearly distinguishable from the iron-produced fragments, among which the most prominent and identically present is a 70-kDa band (Fig. 1*B, 3rd* and *4th lanes*).

To map the nucleotide-binding site(s), we performed protein footprinting experiments with anti-Hsp90 antibodies raised against the C or N terminus, respectively. For the sake of consistency, fragments are labeled by C or N (indicating the intact terminus) and a number denoting the apparent molecular weight. Although ADP produced only one prominent fragment, C70 (Fig. 1*C, 1st lane*), corresponding to the 70-kDa band, ATP induced three additional fragments, C73, C65, and C36 (Fig. 1*C, 2nd lane*). Under these strict cleavage conditions, only fragments with terminal residues coordinating the iron-phosphate complex are seen, so the difference between the ATP- and ADP-induced cleavage is caused by the ATP γ-phosphate, coordinated by an extreme N-terminal segment (C73) and another segment from the middle domain (*C36*, Fig. 1*C*). In other experiments only the overall amount of fragmentation increased as a function of time or concentration of ATP/ADP, but the proportion of the different fragments was constant, excluding the possibility of differential kinetics in fragmentation.[2]

The specificity of the affinity cleavage has been confirmed several ways. First, excess magnesium or preincubation with SDS abolished the cleavage. Second, the free radical scavenger, glycerol did not affect the specific fragmentation,[2] pointing out a highly specific, protein structure- and metal-nucleotide complex-dependent interaction at the binding site. However, the most rigorous test was a competition experiment. Geldanamycin (GA, 36 μM), a specific antagonist of the N-terminal ATP-binding site (14), completely inhibited the N-terminal fragmentation and did not affect the iron-specific bands (Fig. 1*C, 3rd* to *5th lanes*). In the simultaneous presence of GA and ATP (but not in the presence of
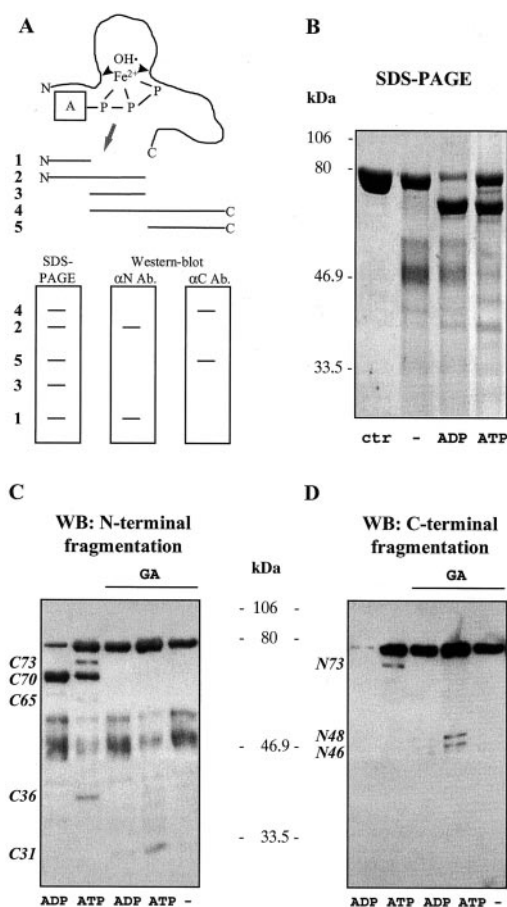

FIG. 1. **Nucleotide affinity cleavage of Hsp90.** *A*, scheme of the reaction (*fragments 1–5* are simply for illustration and do not relate to the experimental fragments). Hsp90 was preincubated in the absence or presence of 36 μM GA at 4 °C for 30 min and then ATP or ADP was added (at final concentrations of 1 or 0.2 mM, respectively), and samples were incubated with a redox system as described under "Experimental Procedures" (*ctr*, untreated protein without ferrous chloride). Gels were either silver-stained (*B*) or blotted and probed with antibodies against the C- (K3725B, C) or the N terminus (K41218, *D*). Experiments were repeated at least three times with similar results. *Ab,* antibody; *WB,* Western blot.

GA and iron), one C-terminal (*C31* Fig. 1*C, 4th lane*) and two N-terminal (*N48* and *N46*, Fig. 1*D, 4th lane*) fragments appeared, suggesting that a second ATP-binding site exists in the C-terminal domain, which becomes accessible only when the N-terminal ATP-binding site is occupied. The reason why we cannot see these additional fragments with ATP preincubation lies in the fact that the Fe^{2+}-ATP-complex initiates an instant cleavage of the N terminus, leaving no chance for the unmasking of the C-terminal ATP-binding site. On blots with higher exposure or a higher amount of protein three additional minor fragments (C39, N38, and N39) could also be detected, but the C-terminal cleavage could not be seen, suggesting that ATP is unable to bind first to the C terminus. C-terminal binding occurs only after the N-terminal binding site is filled (but not cleaved). Experiments with another N-terminal ATP antagonist, radicicol (15, 16), gave similar results.[2] Replacing ATP with the poorly hydrolyzable analogue, ATPγS, induced the appearance of the same fragments both at the N- as well as the C-terminal binding site, however, at approximately 10-fold lower concentration than ATP.[2] Dithiothreitol at 10 mM could selectively compromise the nucleotide binding to the C terminus, raising the possible involvement of reactive cysteines in binding or achieving the binding-competent state (32).[2]

ATP Interacts with the Hsp90-Geldanamycin Complex—Al-
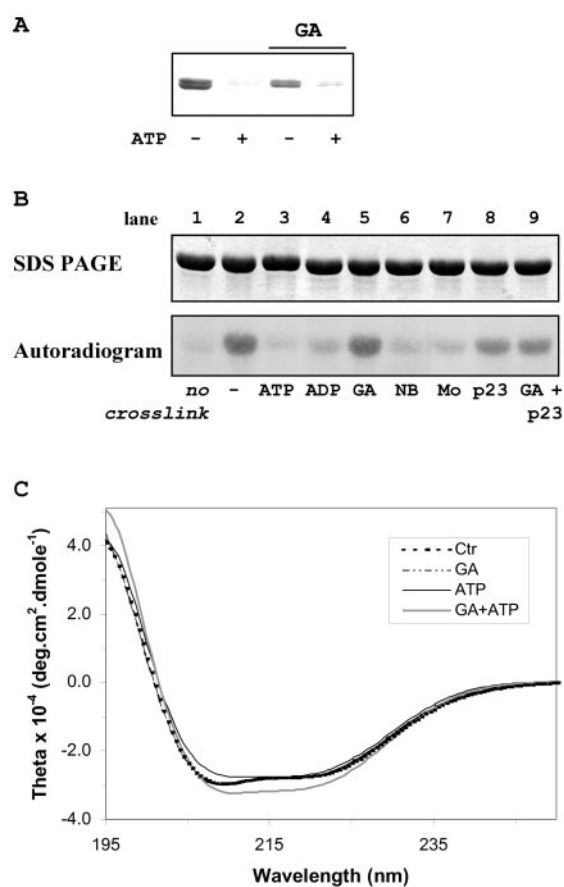
FIG. 2. **Simultaneous binding of GA and ATP to Hsp90.** *A*, binding of Hsp90 to ATP-Sepharose. Hsp90 was preincubated in the absence or presence of 36 μM GA at 4 °C, and then an ATP-regeneration system was added to half of the samples, and their binding to ATP-Sepharose was analyzed as described under "Experimental Procedures." Gel is representative of three independent experiments with similar results. *B*, Hsp90 photoaffinity labeling by [α-^{32}P]ATP. After a 15-min preincubation with ATP, ADP, GA, NB, molybdate, or p23 (at final concentrations of 10 mM, 5 mM, 36 μM, 10 mM, 20 mM, and 0.1 mg/ml, respectively), 0.2 mM [α-^{32}P]ATP was added to all samples, and samples were further incubated for 30 min at 37 °C. UV irradiation was performed for 30 min on ice as described under "Experimental Procedures." Experiments were repeated three times with similar results. *C*, far UV-CD spectra of Hsp90. Hsp90 was preincubated in the absence or presence of 18 μM GA and/or 1 mM ATP for 15 min at 25 °C, and then CD spectrum was recorded according to "Experimental Procedures." Spectra are averages of three experiments.

though the affinity cleavage experiments strongly supported our initial hypothesis of two cooperative nucleotide-binding sites (21), we felt necessary to examine the phenomenon by independent approaches. The γ-phosphate-linked ATP-Sepharose binding assay gave the first biochemical demonstration of Hsp90 N-terminal ATP binding (6). By using this approach Hsp90 bound to the resin in an ATP-competable manner (Fig. 2*A, lanes 1* and *2*), but even very high concentrations of GA inhibited Hsp90 binding by only 60% (Fig. 2*A, lane 3*). Because the K_D value for GA is around 1 μM, at 36 μM GA the N-terminal site is fully saturated; therefore, any further specific ATP binding to this site can be excluded. Specificity was ensured by a complete competition with free ATP (Fig. 2*A, lane 4*) or ATPγS,[2] further substantiating the presence of a GA-independent ATP-binding site.

It should noted that Felts *et al.* (33) could not detect ATP-Sepharose binding of full-length chicken Hsp90α in the presence of GA. In our hands 3–4 washes substantially decreased the low affinity C-terminal binding in the presence of GA,[2] so to preserve the low affinity (but ATP-competable specific) bind-

ing, we applied two washes. As another reason for the discrepancy, we carried out the incubations at 37 °C (instead of 30 °C) (6) because of the higher temperature sensitivity and lower affinity of the C-terminal ATP-binding site.[3] More importantly, we omitted dithiothreitol from the assays because the C-terminal site is sensitive to dithiothreitol.[3] Finally, although we analyzed the binding of rat Hsp90 (β), Marcu *et al.* (20) could detect a C-terminal ATP binding by studying ATP-Sepharose binding of recombinant chicken Hsp90α constructs. This binding was specific and could be inhibited by ATP or GTP. Moreover, they did not include dithiothreitol in the binding buffer either. These and the other independent experiments support the reliability of our results without questioning the accurate work of Felts *et al.* (33).

Our other independent approach has been widely used to detect protein-nucleotide interactions. Upon UV illumination, photolysis of the purine ring of ATP generates covalent adducts with adjacent side chains of the protein. By using radioactive isotope binding, the covalent adduct can be directly visualized after separation from the unbound nucleotide (24). A representative experiment is shown in Fig. 2*B*. Hsp90 was cross-linked with [α-^{32}P]ATP (Fig. 2*B, lane 2*). Cross-linking was prevented by preincubation with cold ATP, ADP, NB, and molybdate (Fig. 2*B, lanes 3, 4, 6,* and *7,* respectively) but not with GA (Fig. 2*B, lane 5*; GA was not destroyed by the UV light, not shown). Interestingly, p23 induced a slight inhibition of [α-^{32}P]ATP binding, which was not further affected by GA (Fig. 2*B, lanes 8* and *9*). The interference of molybdate binding with the N-terminal ATP-binding site is in agreement with its competition with GA (34).

Because Hsp90 undergoes a conformational change upon ATP binding (8), we next investigated the GA- and GA + ATP-induced changes in the far UV-CD spectrum of the chaperone (Fig. 2*C*). The CD spectra observed in control and ATP-containing samples are similar to those reported before (8, 35). GA did not affect the CD spectrum, whereas the addition of ATP to the GA-treated sample had a deep impact on the secondary structure, indicating at least three distinct conformations: the empty, or GA(or ADP)/empty-bound (9, 10), the ATP/ATP-bound, and the GA(or ADP)/ATP-bound state, where the first ligand refers to that of the N-terminal site and the second to that of the C-terminal site, respectively.

Direct Demonstration of Two Distinct ATP-binding Sites of Hsp90—The above-mentioned experiments provided a basis for the existence of a low affinity, geldanamycin-insensitive C-terminal ATP-binding site. However, to get quantitative information on C-terminal ATP binding, experiments providing stoichiometry and accurate kinetic parameters were needed. Traditional experiments (equilibrium dialysis, isothermal titration calorimetry, and rapid centrifugal gel filtration) have a high background noise; therefore either can detect high affinity binding or would require a protein concentration exceeding the K_D value. Therefore, we were seeking for methods/conditions where we could selectively detect the bound species without applying any ATP analogues.

Nitrocellulose filter binding assay was successfully applied for the GHKL-type mismatch repair protein MutL (28). Being in a fortunate situation to have a similar ATP-binding fold in Hsp90 with comparable affinity, we performed slot blot filtration experiments. The results are summarized in Fig. 3. Although we have comparable data with GA,[2] to demonstrate and estimate more accurately the C-terminal ATP-binding properties, we used radicicol, which has a 50-fold higher affinity to Hsp90 than GA (36) and fully inhibits the binding of even 10
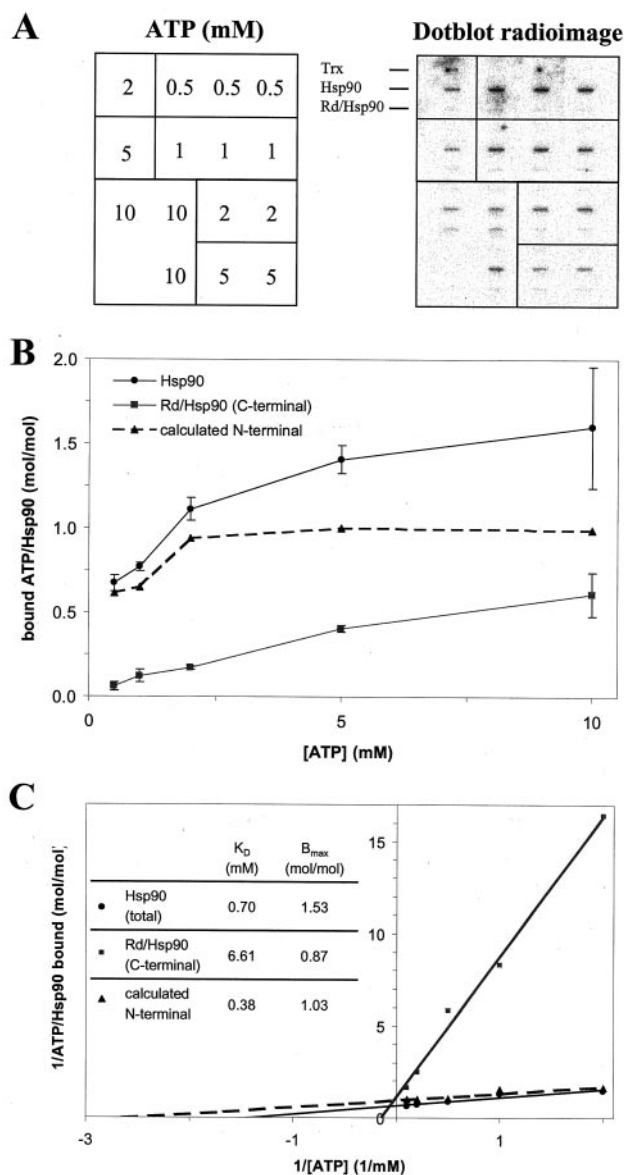
FIG. 3. **Direct demonstration of ATP binding to two distinct sites in Hsp90.** 50 pmol of Hsp90 or thioredoxin (*Trx*) was preincubated in the absence or presence of 60 μM radicicol (*Rd*), and then ATP was added at the indicated concentrations, and bound nucleotide was analyzed by nitrocellulose filter binding as described under "Experimental Procedures." *A*, PhosphorImager scan of a representative slot blot. *B*, ATP binding saturation curves of Hsp90. *C*, double-reciprocal plot and binding constants of the ATP-binding sites of Hsp90. N-terminal nucleotide binding data were calculated by subtracting the residual binding observed in the presence of radicicol from the total binding. Data are means ± S.D. of three experiments.

mM ATP to the N terminus. The calculated parameters of the N-terminal binding site reproduces the earlier experimental data (5, 8, 12), whereas the radicicol-insensitive binding constant agrees with the K_D obtained from affinity cleavage experiments (1–2 mM).[2] Considering the dilution caused by the washing step, it may be overestimated but still in the physiologically relevant range regulating protein function. These experiments also demonstrate that Hsp90 binds two molecules of ATP per monomer.

Mapping the N-terminal ATP-binding Site—Because results presented in Figs. 1–3 demonstrated the suitability of the affinity cleavage reaction to detect nucleotide binding, affinity cleavage studies were extended to map and characterize the ATP-binding sites. C-terminal fragments have different N ter-

---
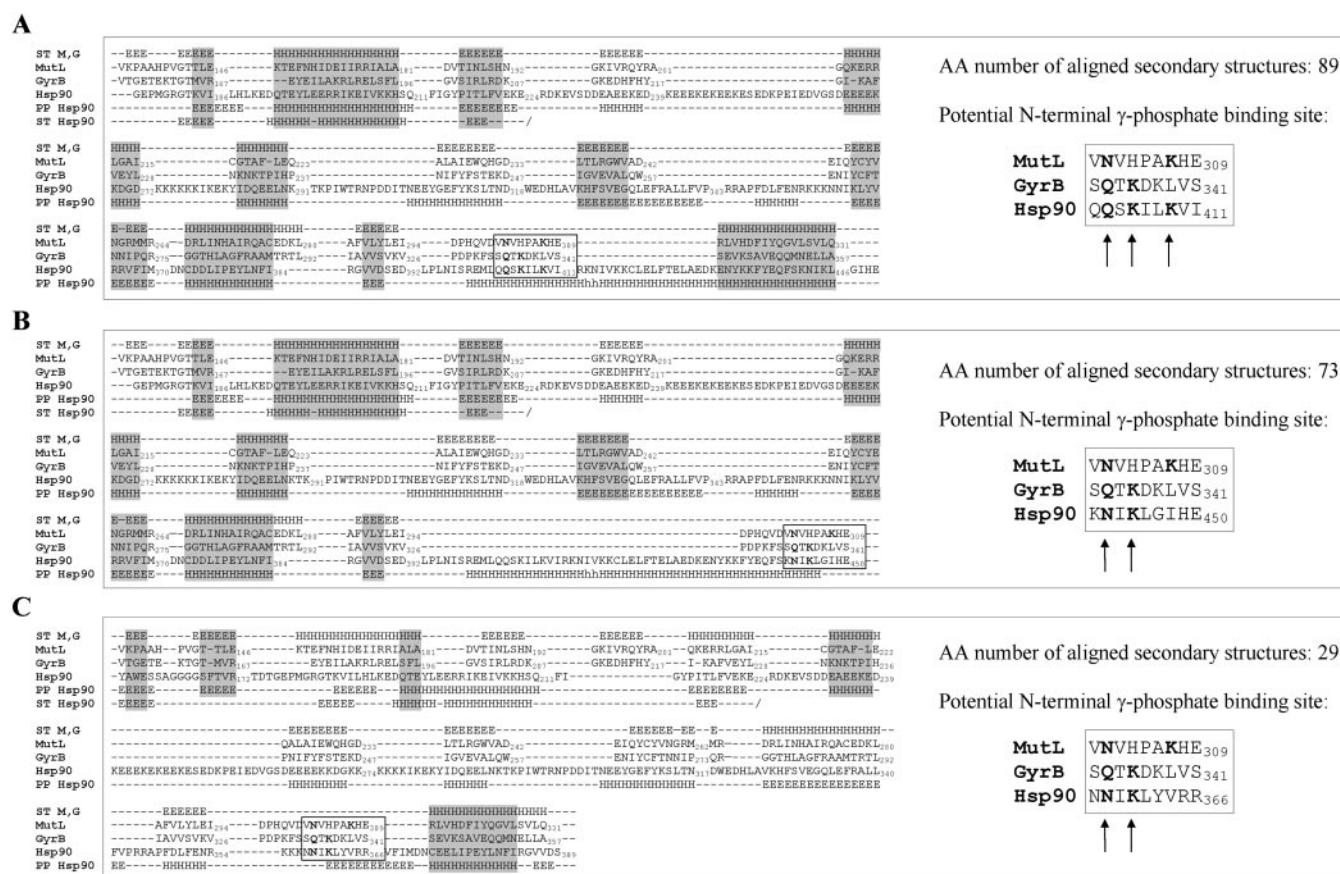
FIG. 4. **Mapping of the N-terminal γ-phosphate-binding site in Hsp90 using secondary structural alignment with GHKL family members.** Candidate γ-phosphate-binding motifs of Hsp90 were selected, and secondary structure predictions were made as described under "Experimental Procedures." Global manual alignments of the secondary structure distributions were made fitting the proteins at the three potential γ-phosphate-binding motifs and are displayed. Matching alignments of 111 (*A*), 95 (*B*), or 116 (*C*) amino acids with helical or extended two-dimensional structures of MutL/GyrB are *highlighted*, and the numbers of aligned amino acids are given on the *right*. The potential motifs are *boxed* and magnified, and the key residues are in *boldface* indicated by *arrows*. *ST M, G*; ST Hsp90: crystal structures of MutL, GyrB, and human Hsp90α, respectively. *PP Hsp90,* PredictProtein prediction for human Hsp90α. *H*, helix; *E*, extended conformation.

mini cleaved at the coordinating residues. To map these residues, fragments were subjected to Edman microsequencing on the blot. C70 yielded a sequence of *XFXV*GFY*XA* corresponding to [119]QFGVGFYSA in yeast Hsp82. This segment is invariable in all Hsp90s, because these are the residues of GHKL motif III (G*XX*G*X*G, see Ref. 13). The preceding Gly[118] contacts the ADP-bound Mg^{2+} through a water molecule and the other glycines bind to the α-phosphate in the yeast Hsp82-ADP complex and also to the γ-phosphate in MutL (28). Sequencing of the other fragments was unsuccessful, due to a potential block of the Edman degradation. Nevertheless, the agreement between the diffraction and affinity cleavage data underlines the accuracy and importance of the in-solution technique yielding information about the nucleotide coordinating segments.

The two functional states of Hsp90 induced by ATP and ADP, respectively, are characterized by major differences, extending beyond the N-terminal domain (7, 9, 37). This suggests a mechanism transducing ATP binding to the subsequent domains. Localization of the γ-phosphate-binding site lying beyond the N-terminal domain can be an important step to elucidate the nucleotide-regulated states of Hsp90.

To localize the γ-phosphate-binding motif of the N-terminal nucleotide-binding site, we performed sequence alignments (pair-wise, multiple, and pattern-defined, see "Experimental Procedures") between MutL, GyrB, and different Hsp90s. First we tried to align Hsp90 with members of the GHKL family (13), but the low sequence identity prevented us from identifying a good candidate motif. Because functional conservation is better

preserved through structural rather than sequence homology, we attempted to find identical secondary structure distribution between the related proteins. Searching for the γ-phosphate-binding pattern of a conserved Lys (Arg) preceded by a conserved Asn or Gln (13), we identified three potential γ-phosphate-binding motifs (we call it motif V) in Hsp90 and, based on the predicted secondary structure of the Hsp90 proteins, aligned them with MutL and GyrB fitting the candidate catalytic motif to the known catalytic motifs of MutL and GyrB. Because crystal structures of the latter proteins include the γ-phosphate-binding residues in the middle domain, we checked the correspondence between the secondary structures, and by far the best alignment came out if the catalytic motifs were matched with the segment at aa ~400 (Fig. 4*A*).

An independent confirmation for the putative γ-phosphate-binding motif comes from studies on the Hsp90 homologue, Trap1 (33). Trap1 binds and hydrolyzes ATP in a GA-sensitive manner. All the motifs I–IV (13) are conserved in Trap1 and prokaryotic Hsp90, HtpG, but the only segment among the motif V candidates, which is conserved both in human and *Drosophila* Trap1 and different HtpG proteins resides in region 400 ([394]QX_5R of *Drosophila melanogaster* Trap and [340]QX_5R of *E. coli* HtpG). Alternatively, only one Arg residue meeting the above criteria and conserved in all Hsp90 proteins could be found ([396]N*XX*R) again in region 400.

Because all the potential identified catalytic sites are in the region of 350–450, to get an experimental evidence of the localization, we subjected the same blot to the anti-C-terminal
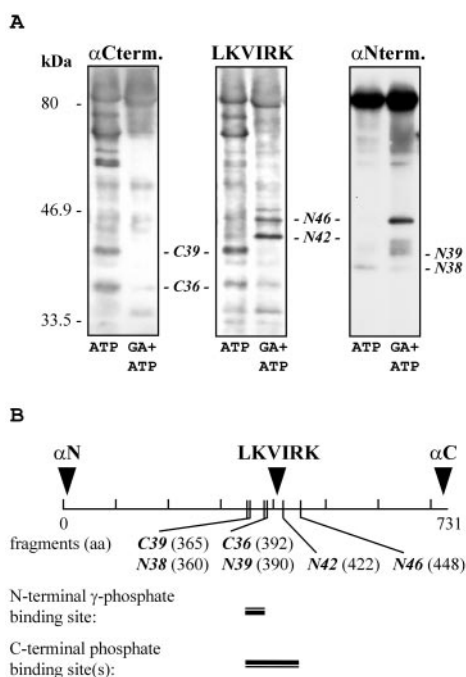
FIG. 5. **Antibody mapping of nucleotide-binding sites in Hsp90.** *A*, affinity-cleaved Hsp90 was blotted, and to identify accurately the fragments, the same blot was probed sequentially with antibodies against the LKVIRK epitope (aa 408–413 (38)), the C terminus (K3725B), and the N terminus (PA3-012). Note that the LKVIRK antibody recognizes numerous fragments and several fragments on the *αC-term*. Blot originates from imperfect stripping. In independent experiments the same was performed with separate blots with the same results. *B*, assignment of the approximate cleavage sites to the fragments based on antibody recognition and on Ferguson analysis of the apparent molecular weight of the fragments. An Hsp90-specific "molecular ruler" calibration curve was obtained by tryptic digestion knowing the major tryptic sites (26, 34).[2] *Numbers* in *parentheses* denote the calculated affinity cleavage sites (±30 aa) of human Hsp90α. Data are representative of three experiments.

K3725B and to the LKVIRK antibody recognizing the highly conserved motif of [408]LKVIRK (38) to see whether it reacts to the C36 fragment. Because this antibody recognizes the C36 fragment (Fig. 5*A, ATP*), C36 should include the LKVIRK epitope (Fig. 5*B*). Accurate molecular weight determinations (see Fig. 5*B* legend) supported these results. Based on these findings and the results of the prediction (Fig. 4), we propose that the γ-phosphate-binding motif is [403]QQsKilK (or [396]NisR).

Mapping the C-terminal ATP-binding Site—The same experimental set up was used to localize the C-terminal nucleotide-induced cleavage sites in Hsp90 (Fig. 5*A, GA+ATP*). Again we subjected the same blot to an anti-N-terminal Hsp90β-specific antibody, PA3-012, and to the LKVIRK antibody. Note that we changed the K41218 antibody used in Fig. 1, which was not isoform-specific and had a lower sensitivity. N48 from Fig. 1 corresponds to the same cleavage site in Hsp90α as N46 does in Hsp90β. The LKVIRK antibody reacts with N46 and N42 but not with N39 and N38. A further refinement based on the site-specific assignment of tryptic fragments (26, 34)[2] yielded the cleavage sites presented in Fig. 4*B* and mapped the C-terminal phosphate-binding motif to the 400 ± 50 aa region. The most intriguing consequence of the localization of both γ-phosphate-binding sites is that the two segments are in close proximity (or may even overlap with each other).

Marcu *et al.* (20) suggested the C-terminal ATP-binding site to be in aa 660–680 by showing that the corresponding deletion mutant did not bind to ATP-Sepharose. To test this by biochemical means, we applied 6 μg of the AC88 antibody (having a recognition site at the region 664–680 (34)), and observed that

it effectively blocked the ATP-induced cleavage in the presence of GA, without altering the N-terminal fragmentation.[2]

Differential Inhibition of the Two ATP-binding Sites—Marcu *et al.* (20) reported a NB-induced inhibition of the C-terminal domain of recombinant chicken Hsp90α binding to γ-phosphate-linked ATP-Sepharose. In their preceding study (19), NB also antagonized the binding of the full-length protein to GA or radicicol beads, whereas GA or radicicol could not affect NB-Sepharose binding. One can predict that NB prevents the binding of ATP to both sites, and indeed, this is illustrated in Fig. 6*A*, where NB abolished the appearance of any specific fragments (*lane 6*), even if GA was also present (*lane 7*). Looking at the NB concentration dependence (Fig. 6*B*), at 1 mM the C-terminal site is already inhibited by 60%, yet the N-terminal site is practically intact. Unfortunately, the overlapping inhibition range of the two sites does not make NB a selective C-terminal-specific agent.

Cisplatin (CP) was reported to bind to the C-terminal 50-aa region (aa 693–731) (35). When Hsp90 was preincubated with 100 μM CP, only the C-terminal ATP-binding was blocked (Fig. 6*A, lanes 9* and *10*) showing that CP may be an important tool to study the role of the C-terminal Hsp90 nucleotide-binding site *in vitro*. Preincubation with NB hindered CP binding and compromised the otherwise intact N-terminal ATP binding (Fig. 6*A, lane 11*).

By having outlined the existence and differential inhibition of two nucleotide-binding sites in purified murine Hsp90, we extended our observations to human recombinant Hsp90α. In all respects, it behaved the same way,[2] indicating the generality of the phenomenon.

Multiple Interactions between the N-terminal and C-terminal Nucleotide-binding Sites—Our previous experiments (Fig. 1) showed that the C-terminal nucleotide-binding site becomes accessible upon N-terminal GA binding. To investigate the requirements for the access to the cryptic C-terminal nucleotide-binding site, we tested the effect of ATP analogues on the cleavage reaction. C-terminal ATP cleavage was detectable in the presence of *ortho*-methylfluorescein phosphate and fluorosulfonylbenzoyl adenosine.[2] These ATP analogues bound to and protected the N-terminal nucleotide-binding site, because in the absence of ATP they could not induce any cleavage. Thus, besides geldanamycin N-terminal binding of ATP analogues is also sufficient to open the C-terminal site.

As a next approach to test the interaction between the two sites, we performed γ-phosphate-linked ATP-Sepharose binding experiments in the absence and presence of excess GA to occupy the N-terminal site in the presence of various nucleotide competitors. As expected, ATP efficiently competed with both N- and C-terminal binding (Fig. 7, *ATP*). ADP at a concentration that is enough to saturate the N-terminal nucleotide-binding site without interfering with the C-terminal binding site did not affect C-terminal ATP binding (Fig. 7, *ADP*). Thus, besides N-terminal ATP, ADP can also induce the C-terminal domain to adopt a conformation able to bind to ATP-Sepharose. GTP does not bind to the N-terminal ATP-binding domain (6)[2] but binds to the C-terminal ATP-binding domain (20).[2] Nevertheless, 5 mM GTP could not completely prevent ATP binding in the presence of GA. However, in the absence of GA GTP caused a 53% inhibition of γ-phosphate-linked ATP-Sepharose binding (Fig. 7, *GTP*), which is more than the expected 34% inhibition corresponding to C-terminal ATP binding (obtained in the presence of GA but in the absence of any other nucleotides). This suggests that C-terminal GTP binding inhibits nucleotide binding to the N-terminal site. Similarly, binding of NB to the C-terminal domain inhibits N-terminal nucleotide binding (Ref. 19 and this study), and molybdate also negatively influ-

A

FIG. 6. **Differential inhibition of the N- and C-terminal ATP-binding sites of Hsp90.** *A*, ATP-induced affinity cleavage in the absence or presence of Hsp90-binding agents. After preincubation of Hsp90 with the compounds in the order indicated *above* the *upper panel* (30 min each at 4 °C; *ctr*, untreated protein, concentrations: 36 μM GA, 10 mM NB, and 0.1 mM CP), affinity cleavage was induced as described under "Experimental Procedures." Blots were probed with Hsp90β-specific anti-C-terminal (K3725B, *upper blot*) and anti-N-terminal (PA3-012, *lower blot*) antibodies. *B*, CP and NB inhibition, concentration dependence. Conditions of the experiment were the same as in *A*. ATP binding was determined in the absence (N-terminal) or in the presence (C-terminal) of GA. Blots were analyzed by densitometry of the C70 (N-terminal ATP-binding) or the N46 (C-terminal ATP binding) fragments, respectively. Experiments were repeated at least three times with similar results. *WB*, Western blot.

B
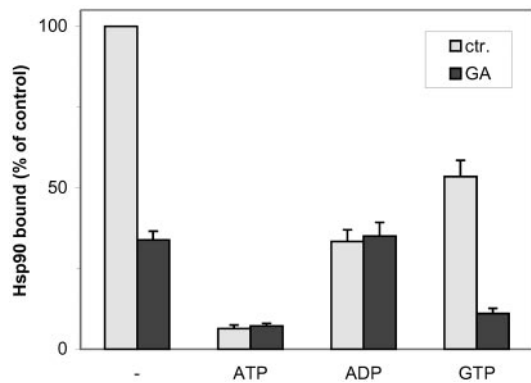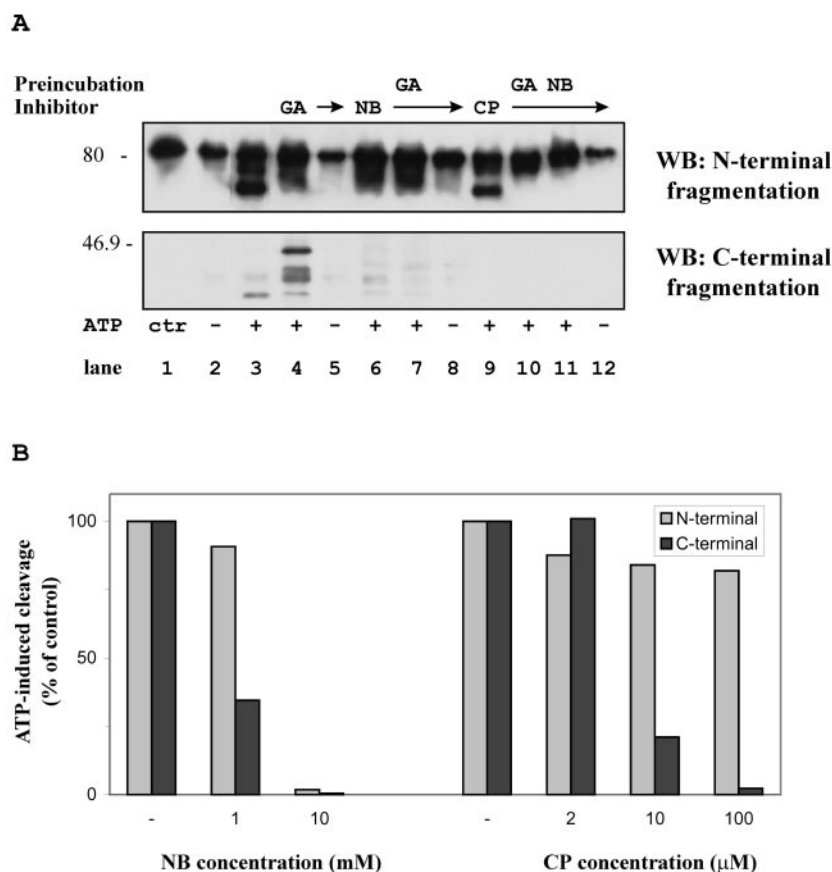
FIG. 7. **Effect of site-selective nucleotides on γ-phosphate-linked ATP-Sepharose binding.** Hsp90 was preincubated in the absence or presence of 36 μM GA at 4°C, then ATP, ADP, or GTP was added at final concentrations of 5, 0.1, or 5 mM, respectively, and incubation was continued for 15 min. Binding to ATP-Sepharose was analyzed as described under "Experimental Procedures." The percent of bound Hsp90 was calculated after a densitometry of SDS-PAGE gels. Data are means ± S.D. of three experiments.

ences the N-terminal ATP binding. Molybdate exerts an effect at the C-terminal domain (34); moreover, the peroxomolybdate-binding site has been suggested to be in the C-terminal domain of Hsp90 (23). Therefore we suggest that the binding site for molybdate itself might be somewhere in the C terminus. It is also intriguing that the C-terminal ATP-binding site is sensitive to dithiothreitol and to cisplatin, both reacting with sulfhydryls. Permolybdate labeling could be inhibited by dithiothreitol (23) and transition-state metals, like vanadate or molybdate, are also reactive to sulfur. Based on these results, it is reasonable to suspect that full-length Hsp90 binds to the γ-phosphate-linked ATP-Sepharose resin through both the N- and C-terminal nucleotide binding domains. Consequently, it

appears that C-terminal nucleotide binding is permitted only if the N-terminal site is charged with either ATP or ADP, and conversely C-terminal ligand binding also regulates N-terminal nucleotide binding.

Effect of the Co-chaperone, p23, on Hsp90 Nucleotide Binding—Substrate release from Hsp90 is dependent on ATP hydrolysis and is stimulated by p23 (39). To assess the functional relevance of ATP-binding sites in Hsp90-protein interactions, we studied the effect of target proteins on the ATP-induced cleavage. Out of several heat- or chemically denatured unspecific substrates tested (citrate synthase, rhodanese, reduced insulin), none had a significant influence on the affinity cleavage induced with or without GA characteristic to the N- and C-terminal nucleotide binding, respectively.[2]

p23 is an important co-chaperone of Hsp90 (1), and its ATP-dependent interaction with Hsp90 is well demonstrated both *in vitro* (9) and *in vivo* (10). Fig. 8 shows a representative blot of the effect of p23 on the nucleotide cleavage reaction. Interestingly, p23 inhibited the N-terminal cleavage (Fig. 8, *lane 5, upper panel*), and at the same time it induced a slight fragmentation in the C-terminal domain (Fig. 8, *lane 5*, *lower panel*), which became even stronger after GA-treatment (Fig. 8, *lane 6, lower panel*). Interestingly, the residual amount of non-cleaved Hsp90 became smaller in the presence of p23 (Fig. 8, *lanes 5* and *6, upper panel*), which might indicate an enhanced fragmentation of Hsp90 in the presence of p23. Molybdate had no major influence on the interference of p23 with the cleavage reaction (Fig. 8, *lanes 7* and *8*). Molybdate alone inhibited nucleotide-induced cleavage at the N-terminal site and to a lesser extent at the C-terminal site (Fig. 8, *lanes 9* and *10*), which is in agreement with our previous data (see Fig. 2*B*). No effect could be observed in the presence of ADP, except that molybdate inhibited its C-terminal binding (Fig. 8, *lanes 11–18*). These results suggest a role for p23 to mediate a confor-

FIG. 8. **p23 shifts the nucleotide state of Hsp90.** Hsp90 was or was not preincubated with 36 μM GA, and then samples were supplemented with 20 mM molybdate and/or 2 μg of p23 as indicated, and incubation proceeded for 20 min at 37 °C. ATP (1 mM) or ADP (0.1 mM in the absence and 1 mM in the presence of GA) was added, and after an incubation of 15 min at 37 °C affinity cleavage was induced as described under "Experimental Procedures." Blots were sequentially probed with antibodies (*Ab*) against the C and N terminus (*ctr*, no affinity cleavage). Gel is a representative of two experiments with similar results.

mational shift of Hsp90 from the "N-terminally active" to a "C-terminally active" state in terms of nucleotide binding.

The C-terminal Nucleotide-binding Site Acts Differently in the Formation of Hsp90-p23 and Hsp90-Hsp70 Complexes— p23 binding requires a dimeric Hsp90 molecule with full capability to bind ATP (6, 37, 40). NB has been shown to disrupt the p23-Hsp90 complex in reticulocyte lysate (20). Based on these findings and on our previous results showing the interference of p23 with the nucleotide binding of Hsp90 at both termini (see Fig. 8), we analyzed the complex formation of these two proteins in the presence of geldanamycin (GA) and cisplatin (CP), inhibitors of the N- and C-terminal nucleotide binding of Hsp90, respectively. In agreement with previous data (9) formation of the Hsp90-p23 complex required ATP and was stabilized by molybdate or by using ATPγS (Fig. 9*A, 1st* to *3rd lanes*), and the complex could be disrupted by GA (*8th* and *9th lanes*). 100 μM CP neither affected complex formation (Fig. 9*A, 4th* and *5th lanes*) nor was able to rescue the complex from the GA-exerted inhibition (*6th* and *7th lanes*). Thus, unlike NB, CP does not affect an N-terminal complex of Hsp90.

GA arrests the glucocorticoid receptor heterocomplex in an intermediate state, in which Hsp90 forms a C-terminal complex with (Hop-)Hsp70 (41). Moreover, Hsp90 can be directly cross-linked to Hsp70, suggesting a weak interaction (42). NB disrupts the Hsp90/Hsc70 association in reticulocyte lysate (20). Therefore, we chose to examine the Hsp90/Hsp70 interaction as another approach to elucidate the functional role of the C-terminal nucleotide-binding site. We immunoprecipitated Hsp70 from Jurkat cells pretreated with different ATP competitors. Rapid and gentle lysis ensured the preservation of native complexes. In control cells, Hsp90 is marginally detected in the Hsp70 chaperone complex (Fig. 9*B, 1st lane*). GA promoted a stronger interaction (Fig. 9*B, 2nd lane*). Surprisingly, CP behaved similarly to GA (Fig. 9*B, 3rd lane*). NB fully disrupted the complex (Fig. 9*B, 4th lane*), giving an *in vivo* confirmation of the *in vitro* data by Neckers and co-workers (20).

DISCUSSION

Our earlier study (4) predicted the presence of a Walker-type ATP-binding site in the middle C-terminal part of Hsp90. At the time of the identification of the N-terminal GHKL-type ATP-binding site (6, 12), several seemingly controversial data have been accumulated in our laboratory, which could have only been rationalized with the existence of more cooperative nucleotide sites with distinct properties (2, 21). To explore the nucleotide-Hsp90 interactions in detail, we set up in-solution techniques allowing us to study the low affinity site(s) under physiological conditions using photoaffinity cross-linking to

FIG. 9. **Effect of cisplatin on Hsp90 complexes.** *A*, cisplatin does not abolish the Hsp90-p23 interaction *in vitro*. Complex formation was allowed to occur, and immunoprecipitation was performed as described under "Experimental Procedures." The *last lane* did not receive p23. GA and CP were used at concentrations of 36 and 100 μM, respectively. *B*, effect of ATP competitors on the Hsp90-Hsp70 interaction *in vivo*. Hsp70 was immunoprecipitated from Jurkat cells treated with 1.8 μM GA, 100 μM CP, or 1 mM NB, respectively. Blots were probed with anti-Hsp90 and anti-Hsp70 antibodies (*ctr*, cells were treated with Me$_2$SO). Treatments did not affect Hsp90 binding to the affinity resin. Experiments were repeated three times with similar results.

freeze the complex in a covalent state, or footprinting Hsp90 at the nucleotide-binding site by oxidative affinity cleavage. The results provided by these experiments are consistent, yet were confirmed and supplemented by the widely accepted ATP-Sepharose binding assay. Nitrocellulose filter binding provided a direct and quantitative demonstration of another geldanamycin/radicicol-insensitive ATP-binding site with physiologically relevant affinity.

Our most important finding is the identification of two separate nucleotide-binding sites in Hsp90 having distinct properties and elaborate interactions. The demonstration that cisplatin is a specific inhibitor of C-terminal nucleotide binding gives a new pharmacological tool to assess nucleotide involvement in Hsp90 function. Similarly, the differential behavior of various Hsp90 partner proteins upon the occupancy of the N- and C-terminal nucleotide-binding sites suggests an important role of both sites in the *in vivo* function of Hsp90.

Nucleotide affinity cleavage mapped the major N-terminal nucleotide-binding motifs in agreement with previous crystallographic data (12, 13). Besides unequivocally identifying the terminus of cleavage fragment C70 as motif III (^{131}GqfGvG) by Edman sequencing, the other motifs can easily be assigned

according to the relative molecular weight of the fragments produced. Fragment C73 may correspond to motif I ([46]ElisNssDA) responsible for ATP hydrolysis (10, 11), whereas C65 may be cleaved at motif IV ([182]GT) known to be involved in GA and p23 binding (6).

In the N-terminal crystal structure the γ-phosphate is not anchored, and we provided the first evidence of the existence of a γ-phosphate-binding motif in the middle domain, analogous to other GHKL family members (13). Careful structural homology search-based alignment combined with experimental data mapped this segment to aa [403]QqsKil(K/R) (or [396]NisR), adjacent to the LKVIRK motif, a highly conserved immunodominant epitope playing a role in invasive candidiasis (38). This motif may be the key element in transducing the nucleotide state of the N-terminal domain toward the C-terminal domain.

Marcu *et al.* (20) located the second C-terminal ATP-binding site to aa 666–679. AC88 antibody binds here (34), and in our hands it blocked ATP cleavage, which gives further support for the involvement of residues aa 666–679 in C-terminal nucleotide binding. γ-phosphate-binding motif of the N-terminal and phosphate-binding motifs of the C-terminal nucleotide-binding sites are located in the middle domain, slightly beyond or

FIG. 10. **Model for the ATP-controlled molecular switch mechanism of Hsp90.** In the absence of ATP, Hsp90 is in an open conformation *[1]*, and the charged region (*black*) binds to the C-terminal domain hindering ATP binding. The first ATP molecule binds to the N-terminal nucleotide-binding site, establishing contacts with the charged region and the γ-phosphate-binding segment (*dotted black*) that enables the C-terminal domain to bind nucleotide *[2]*. Binding of the second ATP results in the closed conformation through the neighboring/overlapping phosphate-binding motifs *[3]*. ATP hydrolysis/release restores the empty conformation. Interactions coming from similar domains of the other Hsp90 molecule of the Hsp90 dimer are not illustrated and cannot be excluded. (The N- and C-terminal nucleotide-binding domains are labeled by *N* and *C*, respectively.)

overlapping with the LKVIRK region. The overlap of the γ-phosphate-binding sites of the N- and C-terminal ATP-binding site reinforces the notion that the two ATP-binding sites are linked both functionally and structurally. Inhibition of C-terminal nucleotide binding by CP does not affect the N-terminal ATP (Fig. 6) and GA binding (Figs. 6*A* and 9*A*), which makes CP a selective C terminal-specific agent.

Communication of N- and C-terminal Hsp90 domains has been suggested by genetic and protein refolding studies (43, 44). Our study demonstrated that in the presence of the N-terminal domain, C-terminal ATP binding demands the occupancy of the N-terminal nucleotide-binding site. Conversely, occupancy of the C-terminal nucleotide-binding site by GTP or NB, but not by CP, inhibits nucleotide binding to the N-terminal site.

Several pieces of experimental evidence support the contact of the charged region with both the N- and C-terminal sites. 1) Marcu *et al.* (20) could only detect C-terminal ATP binding in N-terminal truncation mutants lacking the charged region. Thus, the charged region exerts a permanent inhibition on the C-terminal domain. 2) The charged region modulates the peptide/nucleotide binding of the isolated N-terminal domain (45). 3) Radicicol strongly interacts with the charged region of Grp94 (16). 4) CP also binds at the charged region (beyond aa 276) (35). 5) Besides the whole protein, only the C-terminal domain lacking the charged region is active in luciferase assay (44). Putting together these data, a model can be proposed on the ATP cycle of Hsp90 including the molecular switch function of the charged region (Fig. 10). In the absence of ATP the charged region may form an antiparallel helix pair with a segment of the C terminus, as described before (21) Fig. 10 *[1]*. ATP relieves the steric hindrance and induces a closed conformation (8, 46) (Fig. 10, *[2]* and *[3]*) accompanied by decreased binding to the hydrophobic resin, phenyl-Sepharose (9). Empty conformation is restored by ATP hydrolysis and/or release, but at present it is not known whether there is a separate, C-terminal ATPase in Hsp90. The weak interaction of phosphates with the protein as well as the marginal difference between the ATP and ADP-induced fragmentation may argue against a C-terminal ATPase (Fig. 8).

Besides Hsp90 the only other chaperones having two nucleotide-binding sites are the Hsp100 proteins, which are involved in thermotolerance, ATP-dependent proteolysis, and regulation of genetic and protein-based information (47–49). One of the best-studied representatives of the Hsp100 family is yeast Hsp104, so it is worth comparing its ATP-binding properties to those of Hsp90 (Table I). The comparison opens new areas for further studies, such as characterization of the proposed cooperativity in Hsp90 ATP-binding (21), and examination of the role of Hsp90 N- and C-terminal nucleotide binding in the oligomerization of this chaperone in detail. N-terminal ligands such as GA inhibit the assembly of higher order oligomers at

TABLE I

Comparison of the nucleotide binding properties of Hsp90 and Hsp104

Property	Hsp90		Hsp104	
	NBD1[a]	NBD2	NBD1	NBD2
Nucleotide-binding motif	GHKL	?	Walker	Walker
Ligands	ATP, ADP, CTP	ATP, GTP	ATP, ADP, CTP, UTP	ATP, ?
K_D (mM)	0.2–0.4	6.6	5	0.05
ATPase	Yes	?	Yes	No (?)
Modulators	?	?	Heat, salt, pH, ethanol	
K_M (mM)	0.1–0.8		5	
k_{cat} (min^{-1})	0.3–0.8		200	
Cooperativity	?		Yes	
Role in oligomerization	?	?	Negligible	Indispensable
NBD-NBD communication	Strong		Negligible	

[a] NBD, nucleotide-binding domain.

elevated temperatures (50). On the contrary, other ligands binding and/or affecting the C-terminal domain, such as molybdate (50) or CP,[3] promote the oligomerization of Hsp90, showing a differential influence of the two nucleotide-binding domains on Hsp90 oligomerization.

Cisplatin (*cis*-diamminedichloroplatinum(II)) (CP) is one of the most frequently used chemotherapeutic drugs having an excellent potential against testicular, ovarian, bladder, and other solid tumors (see Refs. 51 and 52 for review). Its primary target is DNA, where CP induces intrastrand (mainly ApG and GpG) and interstrand adducts at micromolar concentration, halting replication, transcription, and finally leading to apoptosis. Nucleophilic groups on proteins can also be targets.

Although Hsp90-p23 complex formation was not changed by the selective C-terminal ATP competitor, CP, Hsp70/Hsp90 interaction was strengthened (Fig. 9). Based on these results alone, it cannot be decided whether CP is an ATP agonist or antagonist. However, any drug, *e.g.* molybdate (34) or AMP-PNP (39) capable of freezing Hsp90 in an unproductive state, impairs Hsp90-dependent processes and inhibits productive cycling of the foldosome. CP, besides inhibiting the *in vitro* chaperone activity of Hsp90 (35), efficiently and selectively blocked C-terminal ATP binding (Fig. 6*B*). Thus, our experiments demonstrated that in addition to the widely used N-terminal ATP blockers, geldanamycin and radicicol, CP can be a novel pharmacological tool to inhibit Hsp90 function, to dissect the N- and C-terminal nucleotide binding of Hsp90, and to explore the role of its C-terminal domain in a wide variety of patho(physiological) processes.

REFERENCES

1. Pratt, W. B., and Toft, D. O. (1997) *Endocr. Rev.* **18,** 306–360
2. Csermely, P., Schnaider, T., Söti, Cs., Prohászka, Z., and Nardai, G. (1998) *Pharmacol. Ther.* **79,** 129–168
3. Buchner, J. (1999) *Trends Biochem. Sci.* **24,** 136–141
4. Csermely, P., and Kahn, C. R. (1991) *J. Biol. Chem.* **266,** 4943–4950
5. Scheibel, T., Neuhofen, S., Weikl, T., Mayr, C., Reinstein, J., Vogel, P. D., and Buchner, J. (1997) *J. Biol. Chem.* **272,** 18608–18613
6. Grenert, J. P., Sullivan, W. P., Fadden, P., Haystead, T. A. J., Clark, J., Mimnaugh, E., Krutzsch, H., Ochel, H. J., Schulte, T. W., Sausville, E., Neckers, L. M., and Toft, D. O. (1997) *J. Biol. Chem.* **272,** 23843–23850
7. Grenert, J. P., Johnson, B. D., and Toft, D. O. (1999) *J. Biol. Chem.* **274,** 17525–17533
8. Csermely, P., Kajtár, J., Hollósi, M., Jalsovszky, Gy., Holly, S., Kahn, C. R., Gergely, P., Jr., Söti, Cs., Mihály, K., and Somogyi, J. (1993) *J. Biol. Chem.* **268,** 1901–1907
9. Sullivan, W., Stensgard, B., Caucutt, G., Bartha, B., McMahon, N., Alnemri, E. S., Litwack, G., and Toft, D. O. (1997) *J. Biol. Chem.* **272,** 8007–8012
10. Obermann, W. M., Sondermann, H., Russo, A. A., Pavletich, N. P., and Hartl, F. U. (1998) *J. Cell Biol.* **275,** 901–910
11. Panaretou, B., Prodromou, C., Roe, M., O'Brien, R., Ladbury, J. E., Piper, W., and Pearl, L. H. (1998) *EMBO J.* **17,** 4829–4836
12. Prodromou, C., Roe, S. M., O'Brien, R., Ladbury, J. E., Piper, P. W., and Pearl, L. H. (1997) *Cell* **90,** 65–75
13. Dutta, R., and Inouye, M. (2000) *Trends Biochem. Sci.* **25,** 24–28
14. Stebbins, C. E., Russo, A. A., Schneider, C., Rosen, N., Hartl, F. U., and Pavletich, N. P. (1997) *Cell* **89,** 239–250
15. Soga, S., Kozawa, T., Narumi, H., Akinaga, S., Irie, K., Matsumoto, K., Sharma, S. V., Nakano, H., Mizukami, T., and Hara, M. (1998) *J. Biol. Chem.* **273,** 822–828
16. Schulte, T. W., Akinaga, S., Murakata, T., Agatsuma, T., Sugimoto, S., Nakano, H., Lee, Y. S., Simen, B. B., Argon, Y., Felts, S., Toft, D. O., Neckers, L. M., and Sharma, S. V. (1999) *Mol. Endocrinol.* **13,** 1435–1448
17. Whitesell, L., Mimnaugh, E. D., De Costa, B., Myers, C. E., and Neckers, L. M. (1994) *Proc. Natl. Acad. Sci. U. S. A.* **91,** 8324–8328
18. Schneider, C., Sepp-Lorenzino, L., Nimmesgern, E., Ouathek, O., Danishefsky, S., Rosen, N., and Hartl, F. U. (1996) *Proc. Natl. Acad. Sci. U. S. A.* **93,** 14536–14541
19. Marcu, M. G., Schulte, T. W., and Neckers, L. M. (2000) *J. Natl. Cancer Inst.* **92,** 242–248
20. Marcu, M. G., Chadli, A., Bouhouche, I., Catelli, M., and Neckers, L. M. (2000) *J. Biol. Chem.* **275,** 37181–37186
21. Söti, Cs., and Csermely, P. (1998) *J. Biosci.* **23,** 347–352
22. Ouimet, P. M., and Kapoor, M. (1999) *Biochem. Cell Biol.* **77,** 89–99
23. Söti, Cs., Radics, L., Yahara, I., and Csermely, P. (1998) *Eur. J. Biochem.* **255,** 611–617
24. Biswas, S. B., and Kornberg, A. (1984) *J. Biol. Chem.* **259,** 7990–7993
25. Alonso, E., and Rubio, V. (1995) *Eur. J. Biochem.* **229,** 377–384
26. Nemoto, T., Sato, N., Iwanari, H., Yamashita, H., and Takashi, T. (1997) *J. Biol. Chem.* **272,** 26179–26187
27. Wong, I., and Lohman, T. M. (1993) *Proc. Natl. Acad. Sci. U. S. A.* **90,** 5428–5432
28. Ban, C., Junop, M., and Yang, W. (1999) *Cell* **97,** 85–97
29. Rost, B., and Sander, C. (1993) *J. Mol. Biol.* **232,** 584–599
30. Rost, B., and Sander, C. (1994) *Proteins* **19,** 55–72
31. Soundar, S., and Coleman, R. F. (1993) *J. Biol. Chem.* **268,** 5264–5271
32. Nardai, G., Sass, B., Eber, J., Orosz, Gy., and Csermely, P. (2000) *Arch. Biochem. Biophys.* **384,** 59–67
33. Felts, S. J., Owen, B. A. L., Nguyen, P. M., Trepel, J., Donner, D. B., and Toft, D. O. (2000) *J. Biol. Chem.* **275,** 3305–3312
34. Hartson, S. D., Thulasiraman, V., Huang, W., Whitesell, L., and Matts, R. L. (1999) *Biochemistry* **38,** 3837–3849
35. Itoh, H., Ogura, M., Komatsuda, A., Wakui, H., Miura, A. B., and Tashiama, Y. (1999) *Biochem. J.* **343,** 697–703
36. Roe, S. M., Prodromou, C., O'Brien, R., Ladbury, J. E., Piper, P. W., and Pearl, L. H. (1999) *J. Med. Chem.* **42,** 260–266
37. Prodromou, C., Panaretou, B., Chohan, S., Siligardi, G., O'Brien, R., Ladbury, J. E., Roe, S. M., Piper, P. W., and Pearl, L. H. (2000) *EMBO J.* **19,** 1–10
38. Matthews, R. C., Burnie, J. P., Howat, D., Rowland, T., and Walton, F. (1991) *Immunology* **74,** 20–24
39. Young, J. C., and Hartl, F. U. (2000) *EMBO J.* **19,** 5930–5940
40. Chadli, A., Bouhouche, I., Sullivan, W., Stensgard, B., McMahon, N., Catelli, M. G., and Toft, D. O. (2000) *Proc. Natl. Acad. Sci. U. S. A.* **97,** 12524–12529
41. Morishima, Y., Kanelakis, K. C., Silverstein, A. M., Dittmar, K. D., Estrada, L., and Pratt, W. B. (2000) *J. Biol. Chem.* **275,** 6894–6900
42. Murphy, P. J. M., Kanelakis, K. C., Galigniana, M. D., Morishima, Y., and Pratt, W. B. (2001) *J. Biol. Chem.* **276,** 30092–30098
43. Scheibel, T., Weikl, T., Rimerman, R., Smith, D., Lindquist, S., and Buchner, J. (1999) *Mol. Microbiol.* **34,** 701–713
44. Johnson, B. D., Chadli, A., Felts, S. J., Bouhouche, I., Catelli, M. G., and Toft, D. O. (2000) *J. Biol. Chem.* **275,** 32499–32507
45. Scheibel, T., Siegmund, H. I., Jaenicke, R., Ganz, P., Lilie, H., and Buchner, J. (1999) *Proc. Natl. Acad. Sci. U. S. A.* **96,** 1297–1302
46. Maruya, M., Sameshima, M., Nemoto, T., and Yahara, I. (1999) *J. Mol. Biol.* **285,** 903–907
47. Schirmer, E. C., Glover, J. R., Singer, M. A., and Lindquist, S. (1996) *Trends Biochem. Sci.* **21,** 289–296
48. Schirmer, E. C., Queitsch, C., Kowal, A. S., Parsell, D. A., and Lindquist, S. (1998) *J. Biol. Chem.* **273,** 15546–15552
49. Schirmer, E. C., Ware, D. M., Queitsch, C., Kowal, A. S., and Lindquist, S. (2001) *Proc. Natl. Acad. Sci. U. S. A.* **98,** 914–919
50. Chadli, A., Ladjimi, M. M., Baulieu, E. E., and Catelli, M. G. (1999) *J. Biol. Chem.* **274,** 4133–4139
51. Zamble, D. B., and Lippard, S. B. (1995) *Trends Biochem. Sci.* **20,** 435–439
52. Jordan, P., and Carmo-Fonseca, M. (2000) *Cell. Mol. Life Sci.* **57,** 1229–1235